Research Journal of Pharmaceutical, Biological and Chemical Sciences

A DFT Study Of The Products Nitration Obtained By The Isocadalene Acylation In Dichloromethane.

Redouan Hammal[1,2]*, Sana El hamidi[3], Hassan El khattabi[2], Ahmed Chekroun[2], Ahmed Benharref[2], and Abdeslam el hajbi[1].

[1]Laboratory of Physical Chemistry, Department of Chemistry, Faculty of Science El Jadida, ChouaibDoukkali University, P.O. Box 20, 24000 El Jadida, Morocco.
[2]Laboratory of Biomolecular Chemistry, Natural Substances and Reactivity, URAC 16, Faculty of Sciences Semlalia, Cadi Ayyad University, P.O. Box 2390, 40000, Marrakech, Morocco.
[3]Laboratory of Materials, Media and Modeling Sciences (LS3M), BP 145. Hassan I University, Polydisciplinaire Faculty, Khouribga, Morocco.

ABSTRACT

In this work, the nitration of the products obtained by the isocadalene acylation is in the context of the development of the most abundant essential oils in Morocco, such as that of Atlas cedar. The [1-(2-isopropyl-4,7-dimethylnaphthalen-1-yl) ethanone] and [1-(2,5-dimethyl-7-isopropylnaphthalen-1-yl) ethanone] reaction in dichloromethane with nitric acid and sulfuric acid is performed at the DFT B3LYP/6-311G(d,p) computational level. Analysis the global indices of reactivity shows that the products obtained by the isocadalene acylation as a nucleophile while the nitronium ion as a electrophile, while Fukui and Parr functions allow to predict a high regioselectivity. The intrinsic reaction coordinate shows that the reaction mechanism can be characterized as "two-step". The transition states were characterized by one and only one imaginary frequency. These results are in good agreement with experimental outcomes.

Keywords: Conceptual DFT; regioselectivity; reactivity index; Transition state theory.

*Corresponding author

INTRODUCTION

This work forms part of our studies into the uses the reactivity of the essential oil of the Atlas Cedar [1-3]. It is one of the raw materials in perfume and cosmetics industry. This oil has been the object of various important studies which focused on the isolation, identification, and reactivity of its constituents [4 - 5].

Nitration is the most widely studied electrophilic aromatic substitution (EAS) in which a hydrogen atom of the aromatic ring is relaced by a nitronium ion. It is the most general process for the preparation of aromatic nitro compounds; and of the part which it has played in the development of theoretical organic chemistry. It is of interest because of its own characteristics as (EAS). Action of a stoichiometric quantity of nitric acid with sulfuric acid on [1-(2-isopropyl-4,7-dimethylnaphthalen-1-yl) ethanone] (note P1) and [1-(2,5-dimethyl-7-isopropylnaphthalen-1-yl) ethanone] (note P2) obtained by isocadalene acylation was used [6] (see figure 1), and analysed the regioselectivity of these reactions.
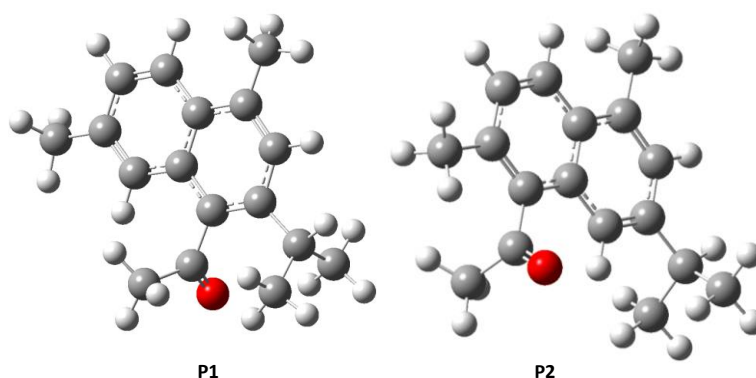

P1   P2

Figure1. The optimized equilibrium structure of P1 and P2**.**

We used chemical potential, global hardness, global softness, electronegativity and electrophilicity in order to predit and to understand the chemical reactivity and site selectivity of the molecular systems has been effectively handled by the conceptual density functional theory (DFT) [7, 8]. Fukui function (FF) [9] and Parr function are very reliable to indicate the site selectivity and local reactivity. The formal definitions of these working equations and descriptors for their computation have been used. In the context of chemical reactivity and site selectivity, the various applications of both global and local reactivity descriptors have been reviewed in detail [10].

Theory and computational details

In order to bring out the nucleophilic/electrophilic character of the reactants, we calculated the electronic chemical potential μ and the global hardness η. These two values can be calculated from the energies of the HOMO and LUMO frontier molecular orbitals, with

$$\mu = \frac{\varepsilon_{HOMO} + \varepsilon_{LUMO}}{2}$$

(1)

$$\eta = \varepsilon_{HOMO} - \varepsilon_{LUMO}$$
(2)

The global electrophilicity index measures the propensity of electron acceptors to acquire an additional electronic charge ΔN from the environment. The electrophilicity [11] is defined as

$$\omega = \frac{\mu^2}{2\eta}$$

(3)

Low values of ionization potential correspond to High values of nucleophilicity and vice versa. Domingo et al. have inserted a relative nucleophilicity index Nu based on the HOMO energies obtained with in the Kohn-Shamscheme [12 - 14] and defined as:

$$Nu = \varepsilon_{HOMO(Nu)} - \varepsilon_{HOMO(TCE)} \qquad (4)$$

This nucleophilicity scale takes tetracyanoethylene as a reference. (TCE) allows us to conveniently handle a nucleophilicity scale of positive values [15, 16].

Fukui Function (FF) is a function that describes the electron density in a frontier orbital, as a result of a small change $\rho(r)$ in the total number of electrons N in the system, at constant external potential $\upsilon(r)$ acting on an electron due to all the nuclei in the system

$$f(r) = \left(\frac{\partial \rho(r)}{\partial N}\right)_{v(r)} = \left(\frac{\partial \mu}{\partial v(r)}\right)_{N} \qquad (5)$$

The condensed FF is calculated using the procedure proposed by Yang and Mortier [17], based on a finite difference method.

$$f_k^{+}(N) = \rho_K(N+1) - \rho_K(N) \qquad \text{for nucleophilic attack} \quad (6)$$

$$f_k^{-}(N) = \rho_K(N) - \rho_K(N-1) \qquad \text{for electrophilic attack} \quad (7)$$

$$f_k^{0}(N) = \frac{1}{2}\left(\rho_K(N+1) - \rho_K(N-1)\right) \qquad \text{for radical attack} \quad (8)$$

Where $\rho_K(N)$; $\rho_K(N-1)$ and $\rho_K(N+1)$ are the gross electronic populations of the site k in neutral, cationic, and anionic systems, respectively. Recently, Domingo et al have proposed that Parr functions P_k as given by the following equations can be used to predict local reactivity [13]:

$$P_k^{-} = \rho_k^{rc} \qquad (9)$$

$$P_k^{+} = \rho_k^{ra} \qquad (10)$$

Where ρ_k^{rc} and ρ_k^{ra} are the atomic spin densities of the radical cation and anion respectively.

When two systems with different electronegativities react together, electrons are transferred from the nucleophilic molecule to the electrophilic molecule until the chemical potentials are equal [18]. The number of electrons transferred ΔNmax is calculated by the following expression [15]:

$$\Delta N_{max} = -\frac{\mu}{\eta} \qquad (11)$$

RESULTS ET DISCUSSION

Analysis of the reactivity indices of the reactants in the base state

The mechanism and selectivity of P1 and P2 nitration has been calculated by DFT methods at the B3LYP/6-311G(d,p) computational level [7, 19]. We calculated the values of enthalpies, entropies and free energies using standard statistical thermodynamics. We analysed the electronic structures of the stationary

points and the bond orders (Wiberg indices) [20] using natural bond order method (NBO) [21, 22]. We identified the ransition states and confirmed their existence by the presence of a single imaginary frequency in the Hessian matrix.

The energy difference between the two possible HOMO/LUMO combinations is given in figure 2,. The energy gap between the HOMO of P1(P2) and the LUMO of NO_2^+ is 0.133 (0.078 eV), while the energy gap between HOMO of NO_2^+ and LUMO of P1(P2) is 13.979 (13.947 eV) indicating that the P1 and P2 products are nucleophiles, while nitronium ion NO_2^+ is an electrophile.

Figure 2: Interaction HOMO/LUMO of the isocadalene and acyl cation calculated by DFT/B3LYP/6-311G(d,p).
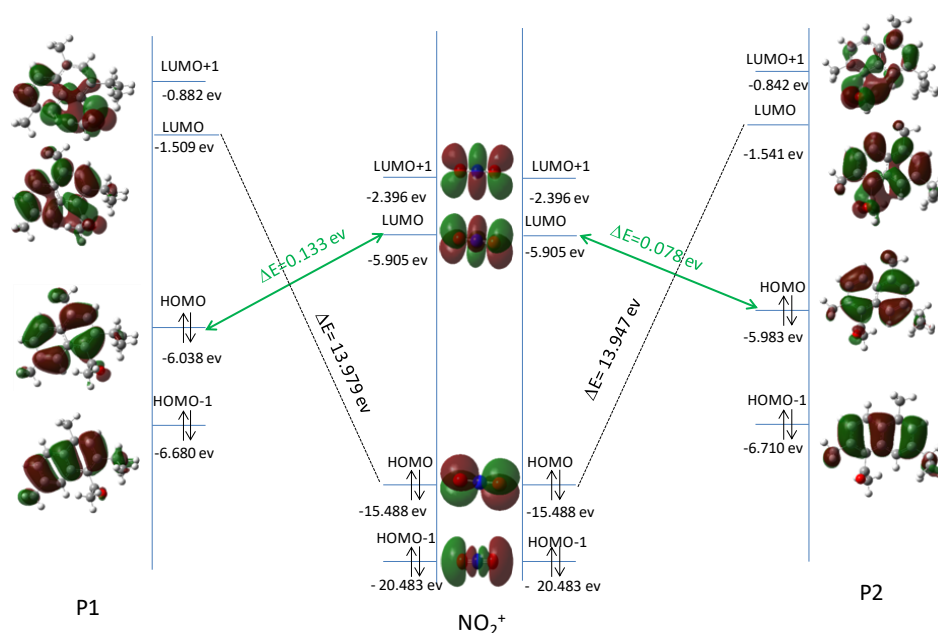
The static global properties, that is, electronic chemical potential μ, chemical hardness η, global electrophilicity ω, global nucleophilicity Nu and global softness S indices, of reagents are reported in Table 1. The electronic chemical potential of electrophile NO_2^+, μ = -11.4395 eV, is lower than that of P1 and (P2), μ = -4.5382 (-3,7622 eV), demonstrating that along a polar nitration reaction path the net charge transfer ΔN will take place from the P1 and P2 toward the nitronium ion. But, the electrophilicity index of electrophile NO_2^+ is 3.6177eV, a value that lies in the range of strong electrophiles on the electrophilicity scale [12], This result justifies that nitronium ion will act as an electrophile will P1 and P2 products will act as nucleophiles, in clear agreement with the ΔN analysis performed at the TS.

Table 1: Electronic global reactivity properties (eV) of nucleophile and electrophile calculated by B3LYP/6-311G(d,p)

	μ	η	ω	Nu	S	ΔN$_{max}$
P1	-4,5382	4,2839	2,4038	2,6885	0,1167	1,0594
P2	-3,7622	4,4420	1,5933	3,3854	0,1126	0,8470
NO$_2^+$	-11,4395	18,0866	3,6177	-6,1193	0,0276	0,6325

In order to predict the most favourable initial electrophile/nucleophile interaction in this nitrationreaction, the nucleophilic f_K^- Fukui functions and P_K^- Parr functions of P1 and P2 and the electrophilic f_K^+ Fukui functions and P_K^+ Parr functions of nitronium ion were analysed.Analysis of the nucleophilic f_K^- and P_K^- of P1 and P2 indicates that the C4 carbon atom is the most nucleophilic centre, $f_{C4}^- = 0.1275$, $P_{C4}^- = 0.2636$, of P1 and $f_{C4}^- = 0.1566$, $P_{C4}^- = 0.3284$, of P2, On the other hand, the electrophilic f_K^+ and P_K^+ of NO_2^+ indicate that the nitrogen atom is the most electrophilic site of this molecule, $f_N^+ = 0.5392$, $P_N^+ = 0.3516$ (see figure 3).
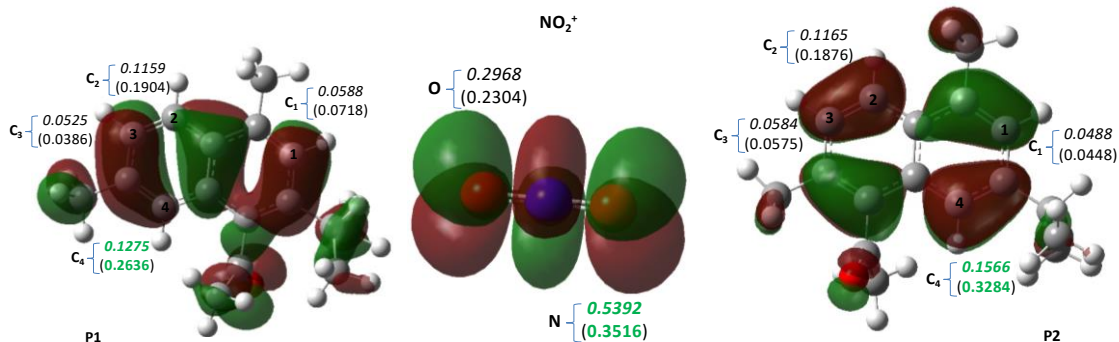
Figure 3: The nucleophilic f_K^- Fukui function and P_K^- Parr functions of P1 and P2 and the electrophilic f_K^+ and P_K^+ of nitronium ion

Consequently, the most favourable interaction between nucleophile and electrophile along the P1 and P2 nitration reaction will take place between the most nucleophilic centre of P1 and P2, the C4 carbon, and the most electrophilic centre of nitronium ion, the nitrogen atom. Furthermore, the most favourable regioisomeric reactive channel will correspond to that associated with the C4-N bond formation, that suggest a high regioselectivity and in good agreement with the experimental outcomes. (scheme 1)

Scheme 1: The reaction path associated with the isocadalene acylation then nitration
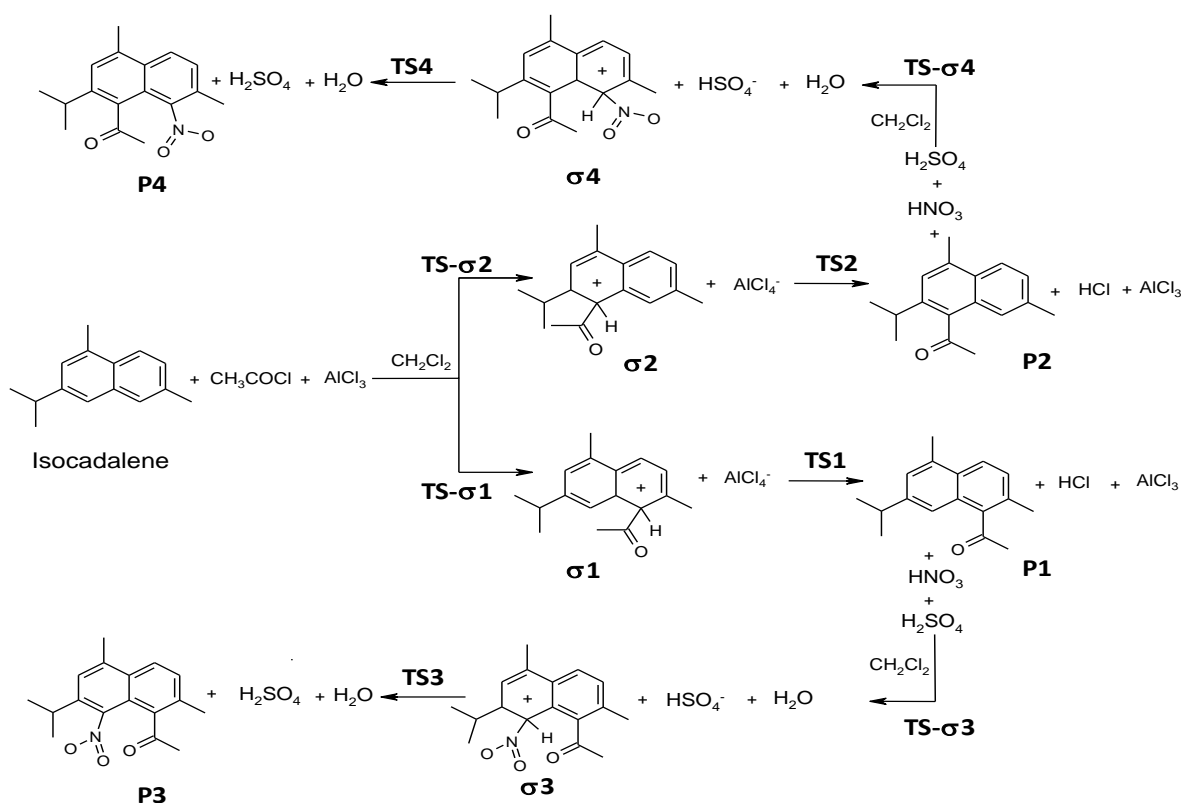
Energy profile and geometry analyses of the P1 and P2 nitration

Energy profile and geometry analyses of the P1 and P2 nitration, we calculated different energy levels in order to show that the nitration preferentially attacked on the C4 position. Figure 4 summarized the total and the relative energies for the EAS reaction of P1 and P2.

The theoretical study of reaction paths and transition states on P1 and P2 nitration allows locating and characterising two TSs (TS-σ3 and TS3) when the attack affects on C4 atom of P1 and two TSs (TS-σ4 and TS4) when it is on C4 atom of P2, thus indicating that it takes place through a two-step mechanism
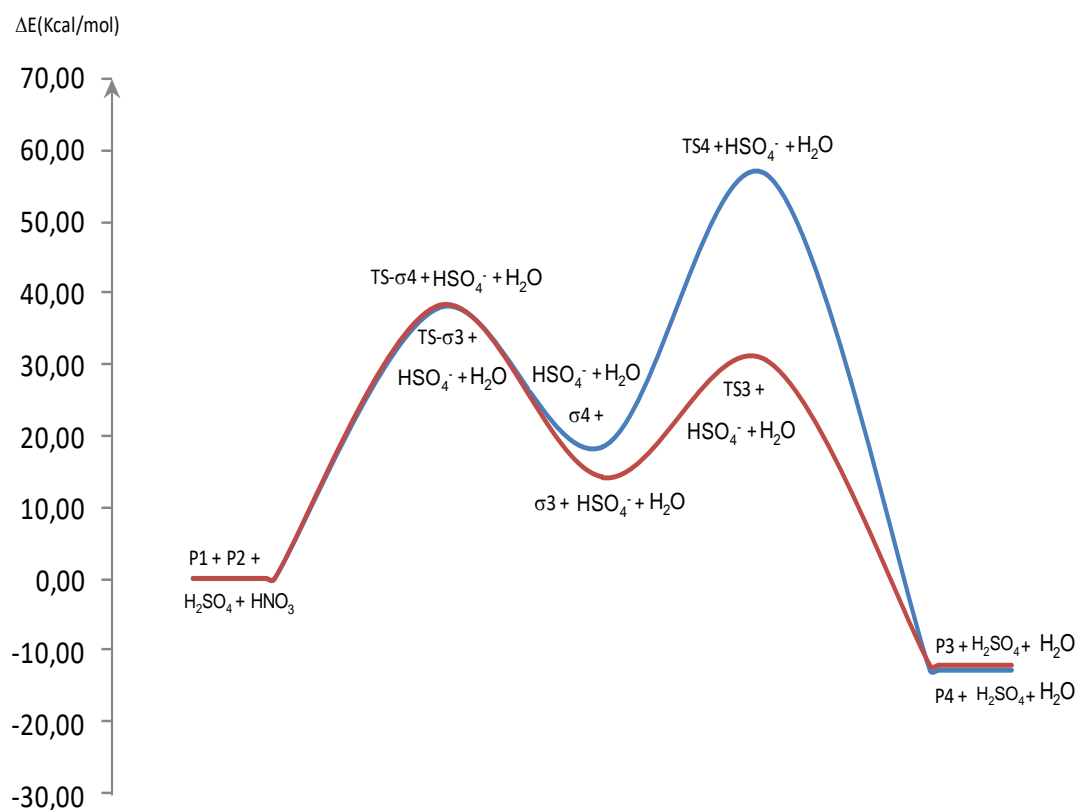

Figure 4: B3LYP/6-311(d,p) relative energy profile of P1 and P2 nitration.

The activation energies of two competitive channels are 38.012 kcal/mol of TS-σ3 (38.068 kcal/mol of TS-σ4), and 56.710 kcal/mol of TS (30.524 kcal/mol of TS4), This nitration reaction is completely regioselective and strongly exothermic; consequently. These energy results shows that the major products P3 obtained for a stoichiometric quantity is formed by kinetic control in good agreement with the experimental outcomes.

The activation energies of σ-complexes are 18.517 and 14.336 kcal/mol for σ3 and σ4 respectively, showing that the formation of σ3, isomer was kinetically preferred. Values of relative thermodynamic energies of the stationary points involved in the P1 and P2 nitration are summarised in table 2.

Table 2: Thermodynamic energies of the P1 and P2 nitration calculated by DFT/6-311G (d, p)

Systèmes	E (u.a)	ΔE (Kcal/mol)	H (u.a)	ΔH (Kcal/mol)	G (u.a)	ΔG (Kcal/mol)
P1	-735,29132		-734,94963		-735,01450	
P2	-735,29478		-734,95336		-735,02076	
HNO$_3$	-280,97316		-280,94235		-280,97254	
H$_2$SO$_4$	-700,33886		-700,29462		-700,32968	
HSO$_4^-$	-699,90318		-699,87095		-699,90530	
H2O	-76,45357		-76,42851		-76,44994	
TS-σ3	-940,18602	38,01221	-939,82980	35,97951	-939,90215	37,23955
TS-σ4	-940,18939	38,06856	-939,83392	33,39857	-939,90650	34,50800
σ3	-940,21709	18,51669	-939,85844	18,01015	-939,93036	19,53563

σ4	-940,22721	14,33603	-939,86820	14,22313	-939,93961	17,65749
TS3	-940,15623	56,70965	-939,802089	53,36969	-939,872896	55,59358
TS4	-940,20141	30,52368	-939,84742	24,92656	-939,91716	27,82064
P3	-939,83119	-12,72084	-939,48459	-13,25488	-939,55479	-11,09688
P4	-939,83373	-12,14816	-939,48690	-12,36445	-939,55667	-8,34839

The P3 and P4 products obtained for a stoichiometric quantity of P1 and P2 nitration are strongly exothermic, by −13.2549 and −12.3645 kcal/mol respectively and exergonic by −11.0969 and -8.3484 kcal/mol respectively. The geometries for different levels of this rection (see figure 5). The length of the N−C4 forming bonds of the TSs associated with the regioisomeric channels 3, are 2.912 Å at TS1−σ3, while at the TSs associated with the regioisomeric channels 4, the distance between the N and the C4 atoms is 2.915 Å at TS1−σ4. The N-C4 bond in the TSs associated with the most favorable P3 channels is the shortest. These geometric parameters suggested an asynchronous bond formation process along the most favorable P3 regioisomer.

The mechanisms for the nitration of acylated products have been calculated by DFT methods at the B3LYP/6-311G(d,p) computational level. The obtained results are supported by the combination of the analysis of the reactivity indices at the ground state of the reagents, derived from the conceptual DFT.
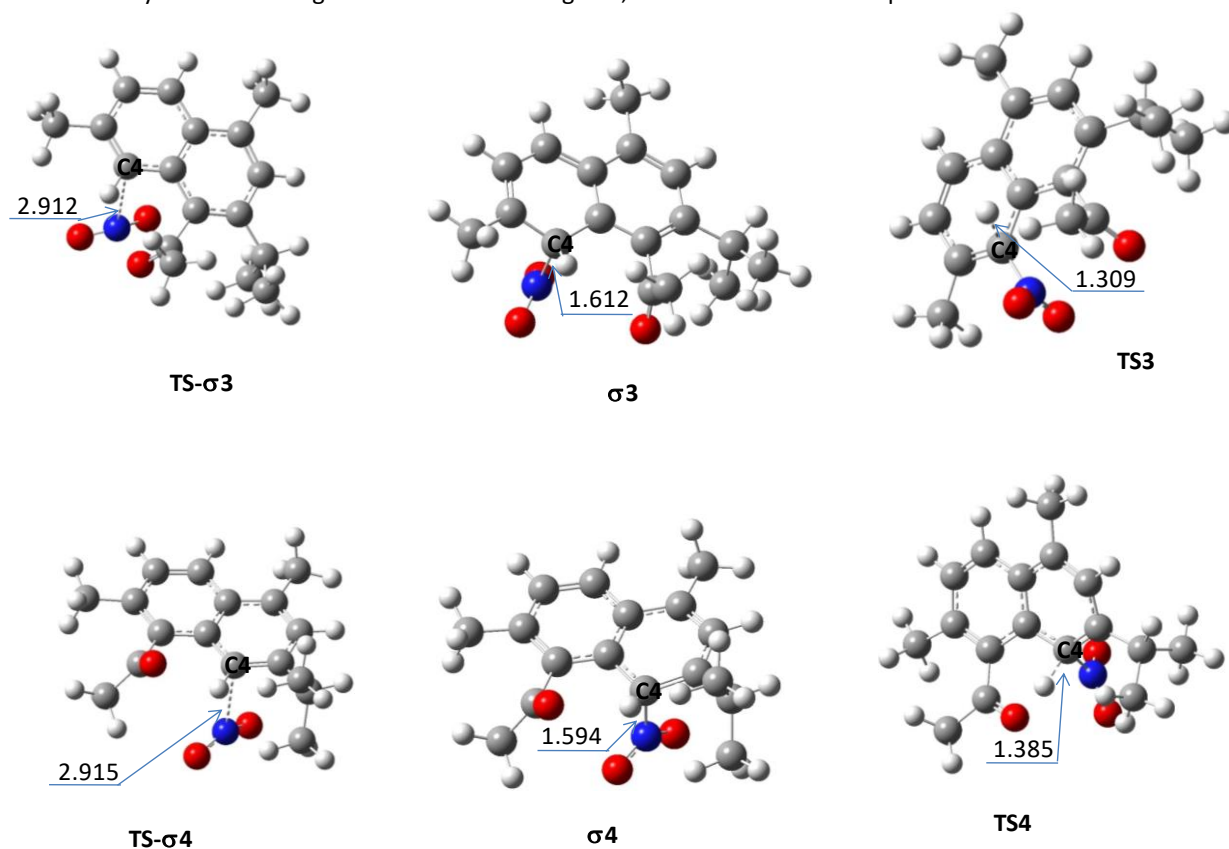

Figure 5: B3LYP/6-311G(d,p) optimized geometries of the TSs involved in the nitration aromatic substitution reactions of P1 and P2. Distances are given in Angstroms

The analysis of the nucleophilic f_k^- Fukui Function and P_k^- Parr functions allows characterising the C4 carbon atom as the most nucleophilic centre of 1-(2-isopropyl-4,7-dimethylnaphthalen-1-yl) ethanone] and [1-(2,5-dimethyl-7-isopropylnaphthalen-1-yl) ethanone], in clear agreement with a high regioselectivity. Calculation of activation energies, analysis of the potential energy surface and the Gibbs free energy indicates that it takes place through a two-step mechanism the nitration of acylated products is thermodynamically and kinetically favored in good agreement with experimental observations.

REFRENCES

[1]   R Hammal., A Benharref., A El Hajbi. International Journal of Innovation and Applied Studies. 6 (2014), 734-745.
[2]   R Hammal., A Zeroual., A Benharref., A El Hajbi.. J. Nat. Prod. Plant Resour. 5 (2015) 6-12.
[3]   R Hammal., A Benharref., A El Hajbi. Journal of Computational Methods in Molecular Design. 5(2015) 16-24.
[4]   M Plattier., P Teisseire. Recherches. 19 (1974) 131-144.
[5]   T C Joseph., Dev Sukh. Tetrahedron. 24 (1968) 3809-3827.
[6]   R Hammal., A Messaoud., M Ait Elhad., A Zeroual., A Benharref., A El Hajbi. Research Journal of Pharmaceutical, Biological and Chemical Sciences. 8 (2017) 477-485.
[7]   C Lee., W Yang., R G Parr. Phys. Rev. B. 37 (1988) 785-789.
[8]   N Shukla., B K Sharma., A Lal and D K Singh. Journal of Chemical and Pharmaceutical Research, 6 (2017) 120-126.
[9]   P W Ayers., M Y Levy. Theor. Chem. Acc. 103 (2000) 353-360.
[10]   P Geerlings., F De Proft., W Langenaeker. Chem. Rev. 103 (2003) 1793-1873.
[11]   R G Parr., L V Szentpaly., S Liu. J. Am. Chem. Soc. 121 (1999) 1922-1924.
[12]   L R Domingo., M J Aurell., P Pérez., R Contreras. Tetrahedron. 58 (2002) 4417-4423.
[13]   L R Domingo., P Pérez., J A Sàez.. RSC Advances. 3 (2013) 1486-1494.
[14]   L R Domingo., E A Chamorro., P Pérez. J. Org. Chem. 73 (2008) 4615-4624.
[15]   R G Parr., W Yang W. J. Am. Chem. Soc. 106 (1984) 4049-4050.
[16]   K Fukui., Science. 218 (1987) 747-754.
[17]   W Yang., W J Mortier. J. Am. Chem. Soc. 108 (1986) 5708-5711.
[18]   P Pérez., L R Domingo., M Duque-Noreña., E A Chamorro. J. Mol. Struc. Theochem. 895 (2009) 86-91.
[19]   A D Becke. J. Chem. Phys. 98 (1993) 5648-5652.
[20]   K B Wiberg. Tetrahedron. 24 (1968) 1083-1096.
[21]   A E Reed., R B Weinstock., F Weinhold., J. Chem. Phys. 83 (1985) 735- 746.
[22]   A E Reed., L A Curtiss., F Weinhold. Chem. Rev. 88 (1988) 899-926.